Unusual Temperature Dependence of Proton Transfer 3. Classical Kramers' Theory versus the Landau−Zener Curve-Crossing Formulation

Boiko Cohen, Pavel Leiderman, and Dan Huppert*

Raymond and Beverly Sackler Faculty of Exact Sciences, School of Chemistry, Tel Aviv University, Tel Aviv 69978, Israel

Received: July 1, 2002; In Final Form: November 21, 2002

Previously, we measured the proton-transfer rate constant from strong photoacids to several solvents such as alcohols and water as a function of temperature. We found an unusual temperature dependence: at high temperature the rate constant is almost temperature independent whereas at low temperature the rate constant exhibits a strong temperature dependence and follows the inverse of the dielectric relaxation time of the particular solvent. We used the Landau−Zener curve-crossing formulation to calculate the proton-transfer rate constant. We explained the temperature dependence as a continuous transition from nonadiabatic (high-temperature) to solvent-controlled (low-temperature) limits. In this study, we used the classical Kramers' theory in the medium and strong-damping limits to calculate the transmission coefficient and rate constant. We found good correspondence between the experimental and calculated proton-transfer rate constant at all temperatures using both models. In both models, the dynamical parameter used to calculate the temperature dependence of the proton-transfer rate constant is the dielectric relaxation time of the particular solvent.

Introduction

In their excited state, photoacids are stronger acids than in their ground state. The excitation of these compounds in a solution of protic solvents enables the study of the dynamics of the proton-transfer reaction from acids to the solvent.[1−6]

In previous papers,[7−10] we described our experimental results of an unusual temperature dependence of excited-state proton transfer from a super photoacid (5,8-dicyano-2-naphthol, DCN2) to several monols, diols, and a glycerol. At relatively high temperatures, the rate of proton transfer is almost temperature-independent whereas at relatively low temperatures the rate exhibits great temperature dependence and the rate constant value is similar to the inverse of the dielectric relaxation time. We also measured the temperature dependence of the proton transfer from two photoacids to water. We chose two photoacids that differ in their acidity in the excited state, pK*, and proton-transfer rate constants. The proton-transfer rate constant, k_{PT}, of the strong photoacid (2-naphthol-6,8-disulfonate, 2N68DS, pK* = 0.4) at room temperature is 2.3×10^{10} s^{-1}. Its temperature dependence in water has similar behavior to that found for DCN2 for several alcohols. At relatively high temperatures, the rate of proton transfer is almost temperature-independent whereas at relatively low temperatures the rate exhibits great temperature dependence. k_{PT}, at room temperature, of the weak photoacid (2-naphthol, 2N, pK* = 2.7) is only 2×10^8 s^{-1}. Its temperature dependence exhibits different behavior. The activation energy of the proton-transfer process is about 12 kJ/mol at high temperatures. At low temperatures, $T < 300$ K, the activation energy increases and reaches $\Delta G^{\ddagger} = 20$ kJ/mol at 250 K.

In our earlier papers,[7,8] we proposed a simple stepwise model to describe and calculate the temperature dependence of the proton transfer to the solvent. The model accounts for the large difference in the temperature dependence and the proton-transfer rate at high and low temperatures. In more recent papers, we explained the temperature dependence of the rate constant for proton transfer to the protic solvent as a continuous transition from nonadiabatic (high-temperature) to solvent-controlled (low-temperature) proton transfer. This phenomenon can be described by the Landau−Zener curve-crossing equation[11,12] for the proton-transfer rate constant.

The development of the theory for the solution-phase proton-transfer reaction is along the lines of electron-transfer theory. It was initiated by Marcus[13,14] as well as Dogonadze, Kuznetzov, Ulstrup, and co-workers[15−19] and then extended by Borgis and Hynes,[20−22] Cukier,[23,24] and Voth.[25,26] These theories suggest that, when a potential energy barrier is present in the proton-reaction coordinate, the reaction pathway involves tunneling through the barrier as opposed to passage over the barrier. The proton transfer can be described as quantum tunneling between two wells formed by two interacting electronic states. The transfer of the proton, from one well to the other, is associated with a change in the electronic state of the system. The crossover between the electronic states can occur only when the proton tunnels through the barrier.

Conventional Landau−Zener (LZ) theory[11,12] provides an accurate description of the process in the absence of interaction with the environment. It is applicable if the motion, in the vicinity of the crossing point, is nearly uniform (ballistic).[27,28] The interaction of the particle with the environment causes complications. The curve-crossing problem in the presence of dissipation has been studied extensively.[29−37] Expressions for the transition rate of various physical limits have been derived.

When the coupling, V, between the diabatic terms is the smallest parameter of the system, the dynamics in the crossing region in this nonadiabatic limit is fast, the tunneling rate is the rate-limiting step, and the reaction rate is given by the Fermi golden rule expression.

When the coupling between the diabatic states is larger than $k_B T$, the adiabatic representation of the coupled potential energy surfaces is adequate, the upper adiabatic potential surface plays

* Corresponding author. E-mail: huppert@tulip.tau.ac.il. Fax/phone: 972-3-6407012.

10.1021/jp026415j CCC: $25.00
Published on Web 02/01/2003

a negligible role, and the rate expression is given by the standard transition-state theory (TST) equation.

Another physical limit is realized when $V \leq k_B T$ and the interaction with the environment is strong enough. The particle spends a "long" time in the crossing-point region. The rate is determined in both the adiabatic and solvent-controlled limits by the dynamics on the lower adiabatic potential surface. The formulation of the problem and the definition of the physical regimes go back to Kramers' theory. In the solvent-controlled limit, the rate is inversely proportional to the solvent relaxation time (friction) and is independent of the coupling V.

In this paper, we use two models to calculate the rate of proton transfer as a function of temperature. We compare the calculation results with the previously published experimental data. The first model is based on classical Kramers' theory[38−40] and its strong relation to solvent friction. The second model is based on the Landau−Zener curve-crossing formulation and was successfully utilized previously to explain the experimental results.

As we shall show, Kramers' theory in the intermediate and strong-damping limit can explain the unusual temperature dependence of excited-state proton-transfer reactions. In the case of the adiabatic or the solvent-controlled limits, the upper adiabatic potential surface plays a negligible role and hence can be treated by Kramers' theory. In Kramers' theory, the dissipative medium (the solvent) is modeled by a thermal bath of harmonic oscillators bilinearly coupled to the system. The strength of the coupling to the bath is usually represented by a damping parameter γ that can be related to the dielectric relaxation of the solvent.

Modeling

A. Classical Kramers' Theory. The standard model for studying reaction rates in solution and general radiationless transitions consists of two crossing diabatic parabolic terms. Radiationless transitions between the terms are induced by the nonadiabatic coupling V. The environment is described in terms of a bath of harmonic oscillators bilinearly coupled to the reaction coordinate.[41]

The dynamics on the lower adiabatic surface is governed by the Hamiltonian of a particle on a potential surface, coupled to the bath, and can be equivalently described in terms of a generalized Langevin equation (GLE):

$$\ddot{q} + \frac{\mathrm{d}U_<(q)}{\mathrm{d}q} + \int^t \mathrm{d}t'\, \gamma(t-t')\, \dot{q}(t') = \xi(t) \qquad (1)$$

$U_<(q)$ is the lower adiabatic potential surface, and q is the system reaction coordinate. The Gaussian stochastic force, $\xi(t)$, has a vanishing mean value and is related to the time-dependent friction function, $\gamma(t)$, via the fluctuation dissipation theorem:

$$\langle \xi(t)\xi(t') \rangle \geq (1/\beta)\gamma(t-t') \qquad (2)$$

with $\beta \equiv 1/k_B T$.

In this paper, we follow the derivation of Rips and Pollak,[36] Rips,[37] and Starobinet et al.[41] In the strong-damping limit, ohmic dissipation holds and is characterized by the friction function

$$\gamma(t) = 2\gamma\delta(t) \qquad (3)$$

In this case, $\hat{\gamma}(s) = \gamma$ is the damping constant (Markovian process).

The reaction rate is determined by the thermally activated classical escape rate of the particle from the reactant well to the product well. In the classical limit, the escape process is thermally activated, and the rate can be written as a product of the Arrhenius factor and an attempt frequency, $\bar{\omega}$:[36]

$$\Gamma = \frac{\bar{\omega}}{2\pi} \exp(-\beta \Delta G^{\ddagger}) = \frac{\omega_0}{2\pi} P \exp(-\beta \Delta G^{\ddagger}) \qquad (4)$$

where P is the dissipative transmission factor, ω_0 is the characteristic frequency of the diabatic potentials, and $\Delta G^{\ddagger}$ is the activation energy. As previously mentioned, we shall limit ourselves to the spatial diffusion limit (γ is independent of time). The transmission factor in this case is determined by the dynamics in the vicinity of the barrier top.

In the limit of small nonadiabatic coupling ($\beta V \ll 1$), the lower adiabatic potential surface, $U_<(q)$, can be modeled as a cusped double-well potential, $U_c(q)$:

$$U_c(q) = \lim_{V \to 0} U_<(q) = \frac{1}{2}\omega_0{}^2 (|q| - q_0)^2 \qquad (5)$$

Calef and Wolynes[31] (CW) suggested using for the transmission factor for the symmetric cusped double-well potential the functional form appropriate for the parabolic barrier. The effective barrier frequency, ω_{eff}, is scaled by the reduced barrier height: $\omega_{\mathrm{eff}} = (\pi\beta\Delta G_*)^{1/2}\omega_0$. Their expression has the form

$$P_c^{\mathrm{CW}} = (2\pi\sigma)^{-1/2}[(1 + 2\pi\sigma)^{1/2} - 1] \qquad (6)$$

where

$$\sigma \equiv 2\beta\Delta G_* (\omega_0/\gamma)^2 \qquad (7)$$

and ΔG_* is the barrier height in the case of a symmetric cusped double-well potential surface.

Rips and Pollak[36] used $\gamma = \omega_0{}^2\tau_L$, τ_L being the longitudinal dielectric relaxation time $\tau_L = (\epsilon_\infty/\epsilon_S)\tau_D$. τ_D is the solvent dielectric relaxation time, and ϵ_∞ and ϵ_S are the high- and low-frequency dielectric constants, respectively.

In the weak-damping limit, this expression reduces to

$$\lim_{\sigma \to \infty} P_c^{\mathrm{CW}} \simeq 1 - (2\pi\sigma)^{-1/2} = 1 - (4\pi\beta\Delta G_*)^{-1/2}(\gamma/\omega_0) \qquad (8)$$

The transmission factor is thus linear in the damping. In the strong-damping limit, the CW expression reduces to Kramers' exact result:

$$\lim_{\sigma \to \infty} P_c^{\mathrm{CW}} \simeq (\pi\sigma/2)^{1/2}[1 - \pi\sigma/2] \qquad (9)$$

We found experimentally[8,9] that the proton-transfer rate constant from a photoacid to solvent at low temperatures scales nicely with the dielectric relaxation time by $k_{\mathrm{PT}}{}^{-1} = \tau_D/b$, where b is an empirical factor determined by the fit of the experimental data and was found to be in the range $4 > b > 1$ for various alcohols and water. Thus, the solvent relaxation time $\tau_S = \tau_D/b$ appropriate for proton-transfer reaction is $\tau_L < \tau_S < \tau_D$.

In this study, we used the following rate constant expression to fit the experimental proton-transfer rate constant as a function of temperature:

$$k_{\mathrm{PT}} = k_{\mathrm{TST}} P_c^{\mathrm{CW}} \qquad (10)$$

and

$$k_{\mathrm{TST}} = \frac{\omega_0'}{2\pi} \mathrm{e}^{-\Delta G^{\ddagger}/RT} \qquad (11)$$

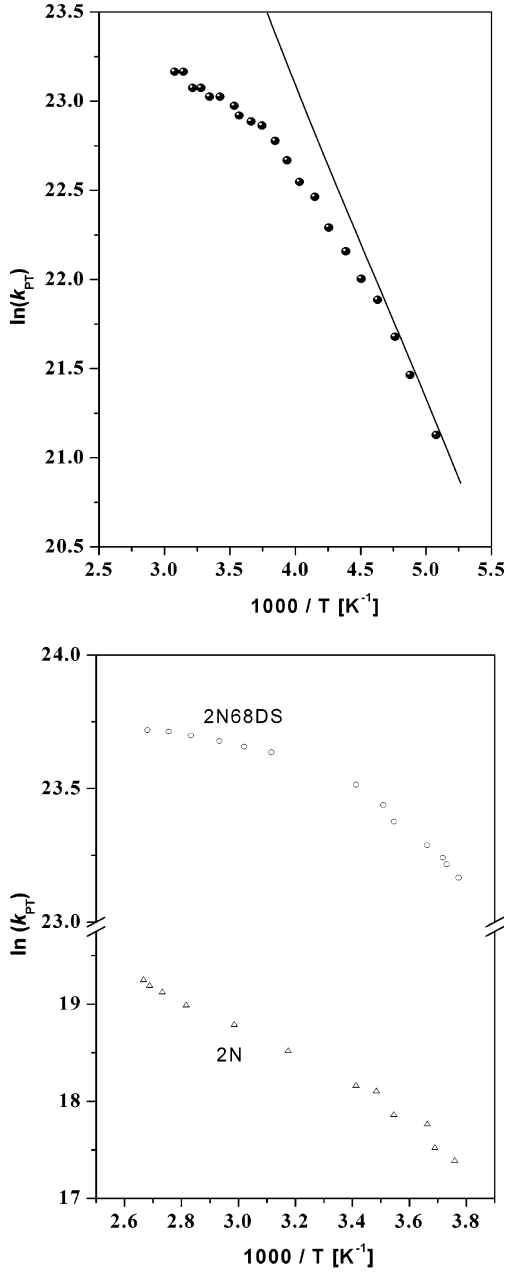

Figure 1. Arrhenius plot of ln k_{PT} versus $1/T$ of the proton-transfer rate constant (a) DCN2 in methanol (●) along with $\tau_S = \tau_D/b$ (—). (b) 2N (△) and 2N68DS (○) in water.

We obtain ω_0' from the high-temperature fit of the experimental data to eq 11.

Figure 1a shows an Arrhenius plot of ln k_{PT} versus $1/T$ of the proton-transfer rate constant from DCN2 to methanol. The slope at the high-temperature limit is small whereas at low temperature the slope is greater. We also plot the inverse of the solvent relaxation time, τ_S^{-1}, for methanol (solid line), which scales with the dielectric relaxation time, to show the good match of the proton-transfer rate constant at low temperatures with τ_D^{-1}. Figure 1b shows an Arrhenius plot of the proton-transfer rate constant from 2N and 2N68DS to water. As can be seen, for 2N the activation energy is also large at high temperatures. The activation energy at temperatures close to the boiling point of water is 12 kJ/mol, and at ~250 K (super-cooled water), it is close to 20 kJ/mol. ω_0' is determined from the high-temperature limit. For 2N68DS in water, we find $\omega_0' \cong 1.8 \times 10^{11}$ s^{-1}, for 2N in water, $\omega_0' \approx 1 \times 10^{11}$ s^{-1}, and for DCN2 in methanol, $\omega_0' = 1.3 \times 10^{11}$ s^{-1}. The value of the rate constant

TABLE 1: Fitting Parameters for the Two Calculation Models

	ω_0' [s^{-1}][a]	V [cm^{-1}][b]	$\Delta G^{\ddagger}$ [kJ/mol][c]	b[d]	τ_D^{298K} [ps][e]
DCN2/MeOH	1.3×10^{11}	2	2.5	2	50
2N/H_2O	0.9×10^{11}	1	12	2	8
2N68DS/H_2O	1.8×10^{11}	2	2.5	2	8

[a] ω_0' is calculated from the high-temperature limit of the experimental rate constant, k_{PT}, and eq 11. [b] Evaluated from the experimental high-temperature rate constant. [c] Activation energy obtained by the best fit to the experimental data. [d] Empirical factor used in the determination of the proton-transfer rate. [e] Dielectric relaxation time at room temperature.

preexponential factor, ω_0', is relatively low compared to the common values used in theoretical considerations and derivations. In his paper, Rips[37] used the ultrafast inertial component of the solvation time-correlation function. For water, he used $\omega_0' \cong 4 \times 10^{13}$ s^{-1}, and for methanol, $\omega_0' \cong 1.5 \times 10^{13}$ s^{-1}. The preexponential factors we find in our studies are closer to the values of τ_D at room temperature than to the ultrafast inertial solvation component. The much smaller preexponential values probably arise from the long-range solvent rearrangements taking place in proton-transfer reactions. The reaction can be described schematically:

$$A^*H\cdots S_B \rightarrow A^{-*}\cdots HS_B^+$$

The reactant is an intermolecular hydrogen-bonded complex between the photoacid, AH^*, and a solvent molecule, S_B, that serves as a base, characterized by a hydrogen bond to the photoacid and other solvent molecules. It was found that this hydrogen bond in protic solvents shifts the fluorescence band of the photoacid to the red by about 1000 cm^{-1}.[42] In water, this specific water molecule, S_B, has three hydrogen bonds to three water molecules. To form the product, $A\cdots HS_B^+$, in water, one hydrogen bond of S_B to a water molecule must break. Thus, relatively long-range reorganization of the hydrogen bond network takes place upon proton transfer to the solvent. This complex rearrangement, to accommodate the product, is probably the reason for a slow solvent-generalized configurational motion that corresponds to a low-frequency component in the solvent dielectric spectrum. Its time constant is close to the slow component of the dielectric relaxation time. The activation energy, $\Delta G^{\ddagger}$, is determined from the high-temperature limit of the slope of the Arrhenius plot of the proton-transfer rate. $\Delta G^{\ddagger}$ at the high-temperature limit for DCN2 in methanol and ethanol, as well as for other alcohols, is relatively low, $\Delta G^{\ddagger} = 2.5$ kJ/mol. Approximately similar values of $\Delta G^{\ddagger}$ are also found for 2N68DS in water.

Figure 2a shows the fit of the experimental data, ln(k_{PT}) versus $1/T$ (solid circles) for the proton-transfer rate constant from DCN2 to methanol, with the calculated rate constant using eq 10. P_c^{CW} is given by eqs 6 and 7. Figure 2b shows the experimental data and fit for 2N in water using the dielectric relaxation data of water and the relatively larger activation energy, $\Delta G^{\ddagger} = 12$ kJ/mol, which we found for 2N in water. Table 1 gives the relevant parameters of the calculation.

B. Landau−Zener Curve-Crossing Formulation. Borgis and Hynes[20−22] derived an expression for the proton-transfer rate constant, k. They wrote an expression for k in a transition-state theory form. k is expressed as the average one-way flux along the solvent coordinate through the crossing point $S^{\ddagger}$ of the two free-energy surfaces, with the inclusion of a transmission coefficient, κ, giving the probability of a successful curve

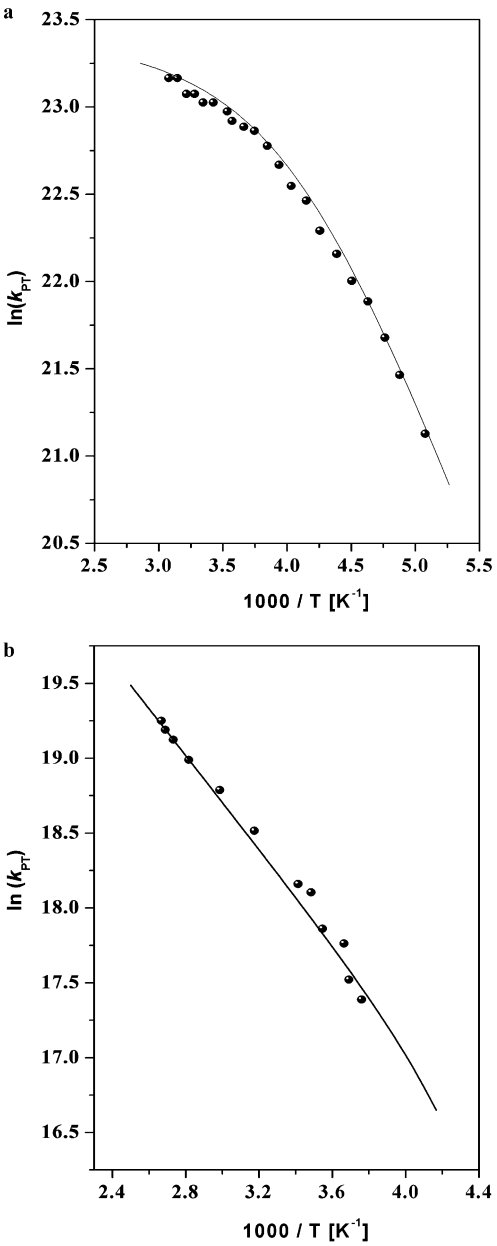

Figure 2. Use of Kramer's theory (—) to fit the experimental data, (full circles) for the proton-transfer rate constant, of (a) DCN2 to methanol and (b) 2N to water.

crossing:

$$k = \langle \dot{S}\Theta(\dot{S})\delta(S - S^{\ddagger})\kappa(\dot{S}, S^{\ddagger})\rangle_{R} \tag{12}$$

where S is the generalized solvent coordinate, $\dot{S}$, the solvent velocity, and $\Theta(\dot{S})$, the step function. The brackets denote averaging over the classical solvent distribution normalized by the partition function of the solvent.

The general Landau−Zener (LZ) transmission coefficient, κ, is given by

$$\kappa = [1 - {}^{1}/_{2}\exp(-g)]^{-1}[1 - \exp(-g)] \tag{13}$$

where

$$g = \frac{2\pi|V|^2}{\hbar\Delta F\dot{S}} = \frac{2\pi|V|^2}{\hbar k_S\dot{S}} \tag{14}$$

is the adiabacity parameter. The expression for the transmission coefficient, κ, includes multiple passage effects on the transition probability. V is the coupling matrix element between the reactant and the product, and ΔF is the slope difference of the diabatic potentials of mean force at the crossing point, $\Delta F = k_S$, where k_S is the parabolic potential surface force constant. When $g \ll 1$, one obtains the nonadiabatic limit result

$$\kappa \cong 2g \tag{15}$$

leading to

$$k_{NA} = \frac{2\pi}{\hbar}|V|^2\left(\frac{\beta}{4\pi E_S}\right)^{1/2}\exp(-\beta\Delta G^{\ddagger}_{NA}) \tag{16}$$

in which $\Delta G^{\ddagger}$ is the Marcus activation free energy

$$\Delta G^{\ddagger}_{NA} = \frac{1}{4E_S}(E_S + \Delta G)^2 \tag{17}$$

The adiabacity parameter g (see eq 14) depends on the potential surfaces' curvature, ΔF, the coupling, $|V|^2$, and the velocity in the vicinity of crossing, $\dot{S}$. $|V|^2$ is independent of temperature. The solvent velocity, $\dot{S}$, however, depends strongly on temperature. In our previous papers, we suggested that $\dot{S}$ is related to the slow components of the solvent relaxation. On the basis of the experimental data, we infer that $\dot{S} = b/\tau_D$, where τ_D is the solvent dielectric relaxation time and b is an empirical factor, dependent on the specific protic solvent, and its value is between 1 and 4.

In the adiabatic limit $V \gg k_BT$, $\kappa \approx 1$, the adiabatic rate expression is

$$k_{AD} = (\omega_s/2\pi)\exp(-\beta\Delta G^{\ddagger}_{AD}) \tag{18}$$

where ω_S is the solvent high frequency and $\Delta G^{\ddagger}_{AD} \cong \Delta G^{\ddagger}_{NA} - V$ is the free energy of activation.

Another physical limit is realized when $V \leq k_BT$ and the interaction with the environment is strong enough. In this solvent-controlled limit, the rate is inversely proportional to the solvent relaxation time (friction) and independent of the coupling V. Rips and Jortner[35] derived an expression for the resonant ($\Delta G^{\ddagger} = 0$) electron-transfer rate in the solvent-controlled limit.

$$k^{ET}_{SC} = \frac{1}{\tau_L}\left(\frac{\beta E_S}{16\pi}\right)^{1/2}\exp(-\beta\Delta G^{\ddagger}_{NA}) \tag{19}$$

For the nonresonance cases, the prefactor in the rate expression (eq 19) changes only by about 20%.

The preexponent depends on the solvent's dynamical properties. At low temperatures, we found that the preexponential factor in the solvent-controlled limit is related to the slowest component of the dielectric relaxation time.We also found that the temperature dependence of the proton transfer can be explained as a continuous transition from the nonadiabatic limit at high temperature to the solvent-controlled limit at low temperature.

A number of attempts have been made to bridge these physical limits. Zusman[29] derived an expression for the rate, bridging the nonadiabatic limit and the solvent-controlled limit. Rips and Jortner have used a simple physical argument to obtain a rate expression that bridges all three limits.[33] They assumed that the crossover could be described in terms of a single dimensionless parameter, the ratio of the mean free path and the root-mean-square displacement of the reaction coordinate.

In our previous papers,[7−10] we used the mean first-passage expression to fit the experimental results. This expression

bridges the nonadiabatic limit and the solvent-controlled limit:

$$k_{PT}(T) = \frac{k_{NA}(T)k_{SC}(T)}{k_{NA}(T) + k_{SC}(T)} \quad (20)$$

where k_{PT} is the overall rate and k_{NA} and k_{SC} are given by eqs 16 and 19.

Numerical Calculation of the Proton-Transfer Rate. For the numerical calculation of the proton-transfer rate constant as a function of temperature, we previously used two crossing parabolic potential surfaces representing the free energy of the reactant and product along the solvent coordinate. The numerical calculation is based on the diffusive propagation of the solvent-generalized coordinate from the equilibrium position of the reactant well to the crossing point. We solve the Debye−Smoluchowski equation (DSE) for the specific problem. The probability density function, $p(S, t)$, to find a solvent configuration S along the generalized solvent coordinate at time t obeys the DSE[29,43,44]

$$\frac{\partial p(S, t)}{\partial t} = D\frac{\partial}{\partial S}e^{-\beta U(S)}\frac{\partial}{\partial S}e^{\beta U(S)}p(S, t) \quad (21)$$

where D is a diffusion constant and $U(S)$ is the potential surface.

In our calculations, we used $E_S = 0.3$ eV for various photoacids either in alcohols or water. The calculation's initial condition is a thermal equilibrium of the probability density function, $p(S)$, of the solvent coordinate of the reactant and is given by a Gaussian distribution centered at the minimum of the reactant well.

The diffusion constant, D, is related to the dielectric relaxation time, τ_D, and the widths of the Gaussian initial distribution,[43] $D = \langle S^2\rangle/2\tau_S$, where $\langle S^2\rangle$ is the mean square displacement and $\tau_S = \tau_D/b$, where b is an empirical factor. For $E_S = 0.3$ eV, $\langle S^2\rangle \cong 0.16$ at room temperature.

The activation energy, $\Delta G^{\ddagger}$, to cross between the reactant well and the product well is determined from the experimental activation energy measured at high temperatures (the nonadiabatic limit). For 2N68DS in water and DCN2 in methanol, we used $\Delta G^{\ddagger} \approx 2.5$ kJ/mol. The position of the activation barrier is determined by $\Delta G^{\ddagger} = U(S^{\ddagger})$ and $S^{\ddagger} = 0.21$. For the weak photoacid 2-naphthol (2N), we used $\Delta G^{\ddagger} \approx 12$ kJ/mol and calculated $S^{\ddagger} = 0.37$.

The next step in the calculation is based upon solving the DSE of a single parabolic potential surface with the relevant initial and boundary conditions. To solve it, we used a modification of the user-friendly graphic program SSDP (version 2.61) of Krissinel and Agmon.[45] The modification is based on the Landau−Zener transmission coefficient κ (eq 13) in the sink term at the crossing point between the reactant well and the product well. The boundary condition at the crossing point is given by

$$\left.\frac{\partial p}{\partial S}\right|_{S=S^{\ddagger}} = -k_0\kappa\frac{b}{\tau_D}p(S^{\ddagger}, t) \quad (22)$$

The boundary condition (eq 22) we chose has components that are similar to those in the expression for the rate constant, expressed in a transition-state theory form (eq 12). The average solvent velocity, $\dot{S}$, is proportional to $1/\tau_D$, κ appears in both expressions, and k_0 is a numerical factor that is independent of temperature and determined by fitting the numerical solution to the experimental proton-transfer rate constant at high temperatures. Finally, the proton-transfer rate constant is obtained from the slope of the plot of $\ln(p)$ versus time.

In Figure 3, we compare the fit to the experimental proton-transfer rate constant, k_{PT}, with the two methods of calculation. The Landau−Zener calculation results were taken from our previous studies.[46,47] Figure 3a shows the Arrhenius plot of ln k_{PT} versus $1/T$ of DCN2 in methanol. We display the proton-transfer rate constant extracted from the experimental data (dots), the calculation based on Kramers' theory (solid line), and the calculation using the Landau−Zener curve-crossing formulation (dashed line). Figure 3b shows the Arrhenius plot of the proton-transfer rate constant of 2-naphthol-6,8-sulfonate to water. The symbols of the experimental data and the two model calculations are the same as in Figure 3a. Figure 3c shows the Arrhenius plot of the experimental and calculated k_{PT} of 2N to water. As seen in Figure 3, both methods of calculation yield a good fit to the experimental results (ln k_{PT} versus $1/T$) of three compounds in two different solvents, which differ in their dielectric relaxation properties. The fitting parameters for both calculation methods are given in Table 1.

Discussion

In this section, we compare the two methods used in this paper to calculate the proton-transfer rate constant, k_{PT}, as a function of temperature. Experimentally, we found that the proton transfer rate from strong photoacids to solvent exhibits an unusual temperature dependence. At high temperatures, k_{PT} is almost temperature-independent whereas at low temperatures it exhibits a strong temperature dependence. At the low-temperature limit, k_{PT} scales with the long component of the dielectric relaxation time, τ_D, of the particular solvent.

Previously, we explained the temperature dependence of k_{PT} as a continuous transition from the nonadiabatic limit (the high-temperature limit) to the solvent-controlled limit (the low temperature limit). We successfully used the Landau−Zener (LZ) curve-crossing formulation to calculate the proton-transfer rate constant at all temperatures.

Three parameters determine the LZ transmission coefficient, κ, (eqs 13 and 14): the coupling matrix element, V, the curvature difference of the diabatic potential surfaces at the crossing point, ΔF, and the solvent velocity at the crossing point, $\dot{S}^{\ddagger}$. We used $\dot{S}^{\ddagger} = b/\tau_D$. From the preexponential factor at the high-temperature limit, we determine the nonadiabatic coupling matrix element (eq 16). For a symmetric reaction where $\Delta G^{\ddagger} = 0$, ΔF can be calculated from the solvent reorganization energy, $\Delta F = 2E_S$, but it is not easy to calculate E_S for proton-transfer reactions. For the proton-transfer rate constant calculations, we chose $E_S = 0.3$ eV independently of the photoacid and the two solvents (methanol and water).

We found that the adiabacity parameter used for the actual best fit of the experimental results, $g_{fit} = g'\tau_D$, is smaller by about a factor of 2−4 from the calculated value, g_{calc} ($g_{fit} < g_{calc}$).

For a known activation energy, Kramers' theory basically has only two parameters, ω_0 and τ_D (or $\tau_S = \tau_D/b$), that determine the proton-transfer rate constant and its temperature dependence. ω_0 is determined from the preexponential factor of the high-temperature limit of the rate constant. We also determine the activation energy of the process at the high-temperature limit.

Comparing the results of the fit with the experimental proton transfer rate of both the weak and strong photoacids to water, we find that ω_0 differs by a factor of 2. (See Table 1.) The computed rate constant follows the temperature dependence of k_{PT} nicely. For the weak acid, k_{PT} also exhibits a large temperature dependence at high temperatures (Figure 3c).

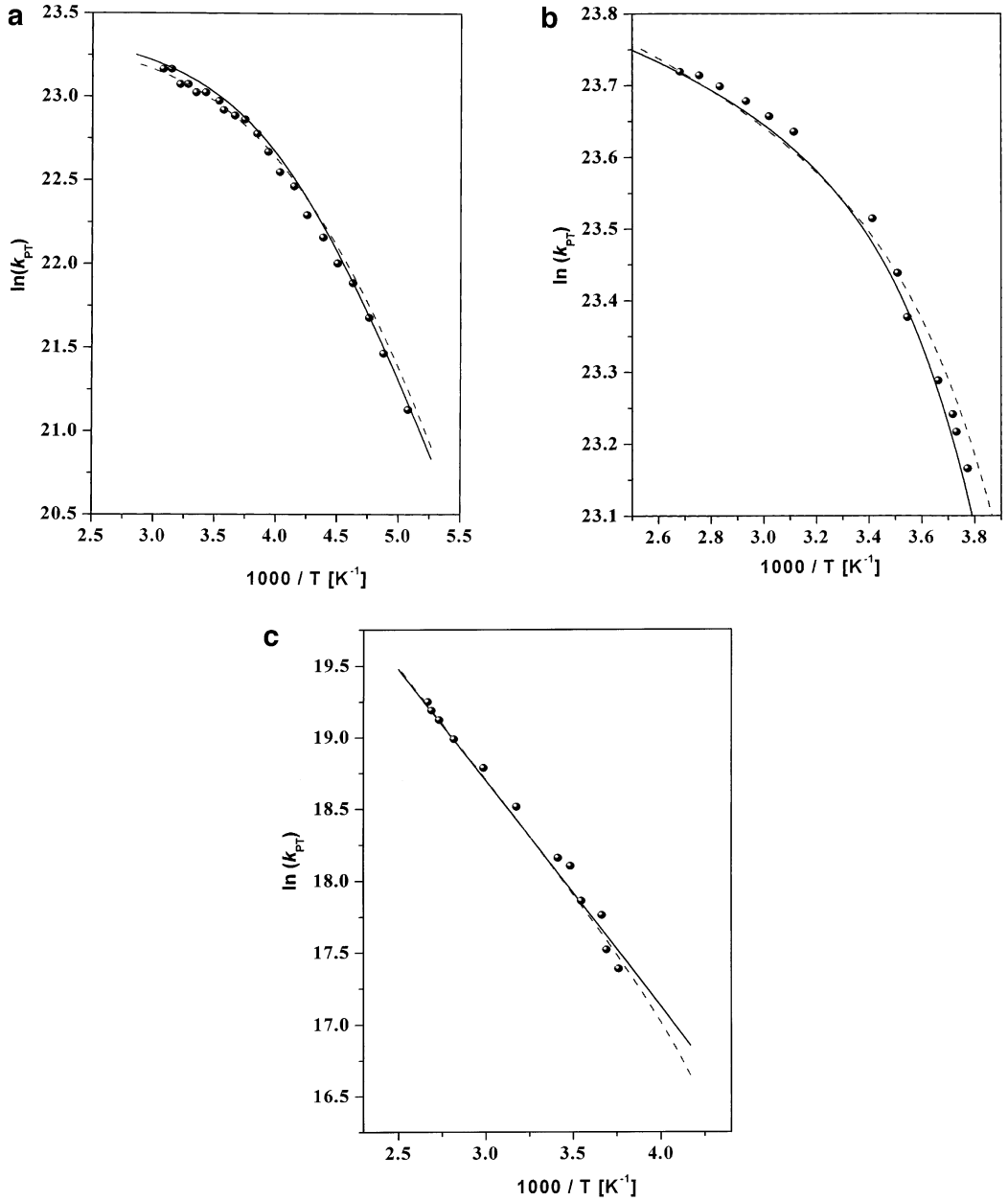

Figure 3. Arrhenius plot of ln k_{PT} versus $1/T$. The proton-transfer rate constant extracted from the experimental data (●), the calculation based on Kramers' theory (—), and the calculation using the Landau−Zener curve-crossing formulation (- -) for (a) DCN2 to MeOH, (b) 2N68DS to water, and (c) 2N to water.

The difference in the quality of the computed fits to the experimental k_{PT}, using the Landau−Zener curve-crossing formulation or Kramers' theory, is not large, and one can use either computation method with almost identical results. The large difference between the two theories lies in their physical origin and assumptions. The LZ transmission coefficient, κ, arises from the quantum nature of the curve-crossing problem whereas the Kramers' transmission factor arises from a classical origin. According to our interpretation of the computational results, using the LZ curve-crossing formulation to fit the experimental data of k_{PT} versus $1/T$, we find that at high temperatures $\kappa_{LZ} < 0.1$ whereas at low temperatures $\kappa_{LZ} \approx 1$. The actual rate constant is small at low temperatures even though the transmission coefficient is close to 1, and since $\langle \dot{S}^2 \rangle^{1/2}$, the root mean square of the solvent coordinate velocity decreases exponentially with the temperature (eq 12) (since τ_D increases exponentially with the decrease in temperature). In Kramers' theory, at the high-temperature limit, the damping constant is in the intermediate region. In this region, the transmission factor, P_c^{CW}, is almost unity and has a very weak temperature dependence. As the temperature decreases, the friction increases and reaches the strong-damping limit. The damping constant, γ, increases exponentially as the temperature decreases, and in the strong-damping limit, the transmission factor, P_c^{CW}, decreases exponentially with the temperature. The proton-transfer rate constant in the strong-damping limit decreases exponentially and follows the dielectric relaxation time.

Electron- and proton-transfer reactions in the condensed phase are described in terms of the transition between two coupled diabatic free-energy surfaces in the generalized solvent configuration coordinate. The model consists of two coupled parabolic diabatic terms with frequency ω_0 and coupling energy V. The interaction between the terms results in an avoided crossing such that the splitting between the two adiabatic potential surfaces is given by $2V$. The dissipative medium is modeled by a thermal

bath of harmonic oscillators coupled to the system. The strength of the coupling to the bath is usually represented by a damping parameter γ.

The influence of the upper adiabatic surface is the main result of the Landau−Zener curve-crossing formalism. When $\beta V < 1$ and the solvent motion is fast, the adiabacity parameter g is small ($g \ll 1$), the LZ transmission coefficient $k_{LZ} \ll 1$, and the rate is determined by the nonadiabatic limit given in eq 16. Under certain conditions, the influence of the upper adiabatic surface can be neglected. This situation is realized when the splitting between the adiabatic surfaces is large compared with the thermal energy ($\beta V > 1$). It can also be realized when the splitting is small ($\beta V < 1$) but the dissipation is strong enough that the particle spends a long time in the crossing-point region (solvent-controlled limit). The rate is determined in these cases by the dynamics on the lower adiabatic potential surface.

We will show that using Kramers' theory in the solvent-controlled limit to describe the dynamics on the lower adiabatic surface and neglecting the upper surface gives similar results for the temperature dependence of the proton transfer rate as determined by the Landau−Zener curve-crossing theory.

To do so, we compare the results of the Landau−Zener calculation with Kramers' theory. As we found in the previous sections, both calculations provide a good fit to the rate as a function of temperature. Rips and Jortner[33] used an interpolation expression for the overall ET rate constant that bridges the two extreme cases, the nonadiabatic and the adiabatic ET. The expression is based on the mean first-passage time (eq 20).

$$k_{et}^{-1} = (k_{et}^{NA})^{-1} + (k_{et}^{AD})^{-1} = \tau_{et}^{NA} + \tau_{et}^{AD} \tag{23}$$

We neglect the small difference in the activation energy of the nonadiabatic and adiabatic rate expressions

$$\tau = (\tau^{NA} + \tau^{AD}) \exp(\beta \Delta G^{\ddagger}) \tag{24}$$

where τ^{AD} and τ^{NA} are time constants equal to the inverse of the prefactors of the rate-constant expression.

$$\tau^{NA} = \frac{\hbar}{2\pi |V|^2} \left(\frac{4\pi E_S}{\beta}\right)^{1/2} \tag{25}$$

$$\tau^{AD} = \tau_L \left(\frac{16\pi}{\beta E_S}\right)^{1/2} \tag{26}$$

τ^{NA} depends on the proton-tunneling coupling matrix element, V, which is unknown and was estimated from the high-temperature limit results and is given in Table 1. It is also dependent, to a lesser extent, on the solvent reorganization energy, E_S. τ^{AD} depends on the solvent longitudinal dielectric relaxation time, τ_L, that depends exponentially on temperature.

The mean first-passage time expression can also be used to present Kramers' theory for arbitrary damping by an equation that bridges between the strong-damping limit and the intermediate-damping case

$$\tau^{CW} = (\tau_1^{CW} + \tau_2^{CW}) \exp(\beta \Delta G^{\ddagger}) \tag{27}$$

where τ_1^{CW} and τ_2^{CW} are the intermediate- and strong-damping limit time-constant expressions, respectively, for Kramers' rate. Using the Calef−Wolynes symmetric cusped double-well potential rate expression, τ_1^{CW} and τ_2^{CW} are given by

$$\tau_1^{CW} = \frac{2\pi}{\omega_{eff}} = \frac{2\pi}{\omega_0} \left(\frac{4}{\pi \beta E_S}\right)^{1/2} \tag{28}$$

$$\tau_2^{CW} = \frac{\omega_0 \tau_L}{\omega_{eff}} = \tau_L \left(\frac{4}{\pi \beta E_S}\right)^{1/2} \tag{29}$$

τ_1^{CW} has a small temperature dependence and depends on the diabatic potential surface frequency, ω_0 . This expression has a similar small temperature dependence to that of τ^{NA} of the Landau−Zener theory, which depends on the coupling matrix element V. In contrast, τ_2^{CW} depends on τ_L, which depends strongly on the temperature as τ^{AD} of the Landau−Zener expression given in eq 26.

Equations 25, 26 and 28, 29 show why both methods of calculating the temperature dependence of the proton-transfer rate constant give similar results if one cannot differntiate between V or ω_0.

In the high-temperature regime, the solvent response is fast (τ_L is small), $\tau^{NA} > \tau^{AD}$, and the overall rate constant of the LZ theory expression is determined by the nonadiabatic rate. In Kramers' theory, at the high-temperature limit, τ_L is small (the damping is relatively small), and τ_2^{CW} is smaller than τ_1^{CW}, hence the overall rate is determined by τ_1^{CW}.

At a low enough temperature, the proton transfer rate is determined in both LZ theory and Kramers' theory by the solvent relaxation since τ_L depends approximately exponentially on the temperature and at a certain low enough temperature $\tau_2^{CW} > \tau_1^{CW}$ and $\tau^{AD} > \tau^{NA}$ and hence the solvent motion controls the rate of proton transfer.

Acknowledgment. We thank Professor I. Rips for his helpful discussions. This work was supported by grants from the US−Israel Binational Science Foundation and the James−Franck German−Israel Program in Laser−Matter Interaction.

References and Notes

(1) Ireland, J. F.; Wyatt, P. A. H. *Adv. Phys. Org. Chem.* **1976**, *12*, 131.
(2) Huppert, D.; Gutman, M.; Kaufmann, K. J. In *Advances in Chemical Physics*; Jortner, J., Levine, R. D., Rice, S. A., Eds.; Wiley: New York, 1981; Vol. 47, p 681. Koswer, E.; Huppert, D. In *Annual Review of Physical Chemistry*; Strauss, H. L., Babcok, G. T., Moore, C. B., Eds. Annual Reviews Inc., Stanford, CA, 1986; Vol. 37, p 122.
(3) Lee, J.; Robinson, G. W.; Webb, S. P.; Philips, L. A.; Clark, J. H. *J. Am. Chem. Soc.*, **1986**, *108*, 6538.
(4) Gutman, M.; Nachliel, E. *Biochim. Biophys. Acta* **1990**, *391*, 1015.
(5) Förster, Th. *Z. Naturwiss.* **1949**, *36*, 186.
(6) Weller, A. *Prog. React. Kinet.* **1961**, *1*, 189.
(7) Poles, E.; Cohen, B.; Huppert, D. *Isr. J. Chem.* **1999**, *39*, 347.
(8) Cohen, B.; Huppert, D. *J. Phys. Chem. A* **2000**, *104*, 2663.
(9) Cohen, B.; Huppert, D. *J. Phys. Chem. A* **2001**, *105*, 2980.
(10) Cohen, B.; Huppert, D. *J. Phys. Chem. A* **2002,** *106*, 1946.
(11) Landau, L. D. *Phys. Z. Sowjetunion* **1932**, *1*, 88; Landau, L. D. *Phys. Z. Sowjetunion* **1932**, *2*, 46.
(12) Zener, C. *Proc. R. Soc. London, Ser. A* **1932**, *137*, 696.
(13) Marcus, R. A. *J. Phys. Chem.* **1968**, *72*, 891.
(14) Cohen, A. O.; Marcus, R. A. *J. Phys. Chem.* **1968**, *72*, 4249.
(15) German, E. D.; Dogonadze, R. R.; Kuznetsov, A. M.; Levich, V. G.; Kharkats, Yu. I. *Elektrokhimiya* **1970**, *6*, 350.
(16) German, E. D.; Kuznetsov, A. M.; Dogonadze, R. R. *J. Chem. Soc., Faraday Trans. 2* **1980**, *76*, 1128.
(17) German, E. D.; Kuznetsov, A. M. *J. Chem. Soc., Faraday Trans. 1* **1981**, *77*, 397.
(18) German, E. D.; Kuznetsov, A. M. *J. Chem. Soc., Faraday Trans. 2* **1981**, *77*, 2203.
(19) Kuznetsov, A. M. Charge Transfer in Physics, Chemistry and Biology Physical Mechanisms of Elementary Processes and an Introduction to the Theory; Gordon and Breach: Amsterdam, 1995.
(20) Borgis, D.; Hynes, J. T. *J. Phys. Chem.* **1996**, *100*, 1118.
(21) Borgis, D. C.; Lee, S.; Hynes, J. T. *Chem. Phys. Lett.* **1989**, *162*, 19.
(22) Borgis, D.; Hynes, J. T. *J. Chem. Phys.* **1991**, *94*, 3619.

(23) Cukier, R. I.; Morillo, M. *J. Chem. Phys.* **1989**, *91*, 857.
(24) Morillo, M.; Cukier, R. I. *J. Chem. Phys.* **1990**, *92*, 4833.
(25) Li, D.; Voth, G. A. *J. Phys. Chem.* **1991**, *95*, 10425.
(26) Lobaugh, J.; Voth, G. A. *J. Chem. Phys.* **1994**, *100*, 3039.
(27) Landau, L. D.; Lifshitz, E. M. *Quantum Mechanics: Nonrelativistic Theory;* Pergamon Press: New York, 1977; Section 90.
(28) Nikitin, E. E.; Umanskii, S. Y. *Theory of Slow Atomic Collisions*; Springer: Berlin, 1984; Chapter 8.
(29) Zusman, L. D. *Chem. Phys.* **1980**, *49*, 295.
(30) Yakobson, B. I.; Burshtein, A. I. *Chem. Phys.* **1980**, *49*, 385.
(31) Calef, D. F.; Wolynes, P. G. *J. Phys. Chem.* **1983**, *87*, 3387.
(32) Frauenfelder, H.; Wolynes, P. G. *Science (Washington, D.C.)* **1985**, *229*, 337.
(33) Rips, I.; Jortner, J. *J. Chem. Phys.* **1987**, *87*, 2090.
(34) Straub, J. E.; Berne, B. J. *J. Chem. Phys.* **1987**, *87*, 6111.
(35) Rips I.; Jortner, J. In *Perspectives in Photosynthesis*; Jortner, J., Pullman, B., Eds.; Kluwer: Dordrecht, The Netherlands, 1990; p 293.
(36) Rips, I.; Pollak, E. *J. Chem. Phys.* **1995**, *103*, 7912.
(37) Rips, I. *J. Chem. Phys.* **1996**, *24*, 9795.
(38) Kramers, H. A. *Physica* **1940**, *7*, 284.
(39) Hänggi, P.; Talkner, P.; Borkovec, M. *Rev. Mod. Phys.* **1990**, *62*, 251.
(40) Nitzan, A. *Adv. Chem. Phys.* **1988**, *70*, 489.
(41) Starobinets, A.; Rips, I.; Pollak E. *J. Chem. Phys.* **1996**, *104*, 6547.
(42) Solntsev, K.; Huppert, D.; Agmon, N. *J. Phys. Chem. A* **1999**, *103*, 6984.
(43) Sumi, H.; Marcus, R. A. *J. Chem. Phys.* **1986**, *84*, 4272. Sumi, H.; Marcus, R. A. *J. Chem. Phys.* **1986**, *84*, 4894.
(44) Agmon, N.; Hopfield, J. J. *J. Chem. Phys.* **1983**, *78*, 6947.
(45) Krissinel, E. B.; Agmon, N. *J. Comput. Chem.* **1996**, *17*, 1085.
(46) Cohen, B.; Segal, J.; Huppert, D. *J. Phys. Chem. A* **2002**, *106*, 7462.
(47) Cohen, B.; Leiderman, P.; Huppert, D. *J. Phys. Chem. A* **2002**, *106*, 11115.